AD-A108 211 SCIENCE APPLICATIONS INC MCLEAN VA F/G 20/4
SPECTRAL MODEL PREDICTIONS OF MEAN-SQUARE-SHEAR DISTORTION RATE--ETC(U)
MAY 81 W GRABOWSKI, F C NEWMAN N00014-81-C-0084
UNCLASSIFIED SAI-82-485-WA NL

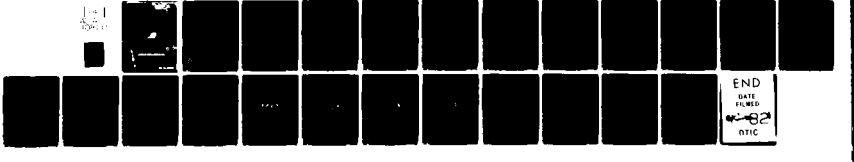

END
DATE FILMED
-82
DTIC

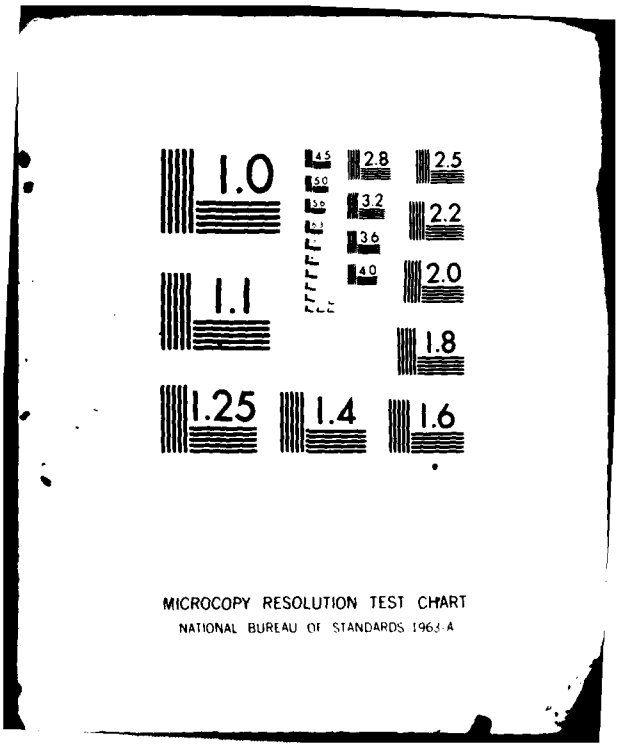
1.0
1.1
1.25
1.4
1.6
1.8
2.0
2.2
2.5
2.8
3.2
3.6
4.0
4.5
5.0
5.6
MICROCOPY RESOLUTION TEST CHART
NATIONAL BUREAU OF STANDARDS 1963-A

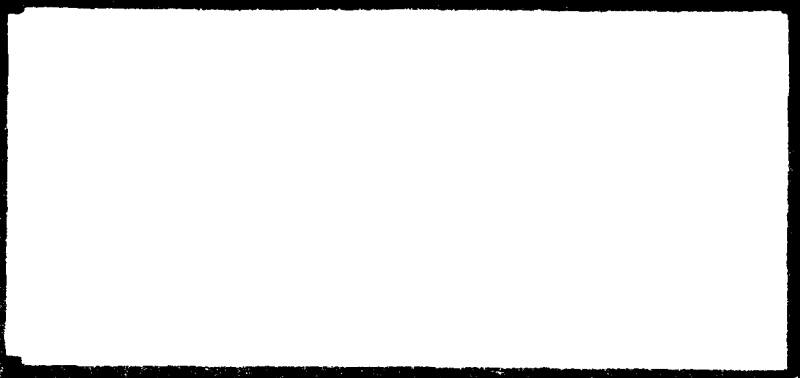

SPECTRAL MODEL PREDICTIONS OF MEAN-SQUARE-SHEAR DISTORTION RATES

SAI-82-485-WA

SPECTRAL MODEL PREDICTIONS OF MEAN-SQUARE-SHEAR DISTORTION RATES

SAI-82-485-WA

OP TN 81-201-01

7 May 1981

Walt Grabowski
Fred C. Newman
Ocean Physics Division

for:
Ocean Measurements Program
Naval Ocean Research and Development Activity
Bay St. Louis, Mississippi 39529

Contracts N00014-81-C-0084
and N00014-81-C-0075

SCIENCE APPLICATIONS, INC.
P.O. Box 1303
1710 Goodridge Drive
McLean, Virginia 22102
(703) 821-4300

SECURITY CLASSIFICATION OF THIS PAGE (When Data Entered)

REPORT DOCUMENTATION PAGE		READ DISTRUCTIONS BEFORE COMPLETING FORM
1. REPORT NUMBER SAI-82-485-WA	2. GOVT ACCESSION NO. AD-A108 227	3. RECIPIENT'S CATALOG NUMBER
4. TITLE (and Subtitle) Spectral Model Predictions of Mean-Square-Shear Distortion Rates		5. TYPE OF REPORT & PERIOD COVERED TECHNICAL 20 Nov 80 - 7 May 81
		6. PERFORMING ORG. REPORT NUMBER SAI-82-485-WA
7. AUTHOR(s) Walt Grabowski Fred Newman		8. CONTRACT OR GRANT NUMBER(s) N00014-81-C-0084 N00014-81-C-0075
9. PERFORMING ORGANIZATION NAME AND ADDRESS Science Applications, Inc. 1710 Goodridge Drive McLean, Virginia 22102		10. PROGRAM ELEMENT, PROJECT, TASK AREA & WORK UNIT NUMBERS
11. CONTROLLING OFFICE NAME AND ADDRESS		12. REPORT DATE 7 May 1981
		13. NUMBER OF PAGES
14. MONITORING AGENCY NAME & ADDRESS(if different from Controlling Office)		15. SECURITY CLASS. (of this report) UNCLASSIFIED
		15a. DECLASSIFICATION/DOWNGRADING SCHEDULE N/A

16. DISTRIBUTION STATEMENT (of this Report)

[redacted]

17. DISTRIBUTION STATEMENT (of the abstract entered in Block 20, if different from Report)

18. SUPPLEMENTARY NOTES

19. KEY WORDS (Continue on reverse side if necessary and identify by block number)

Shear, wake distortion

20. ABSTRACT (Continue on reverse side if necessary and identify by block number)

It is possible to use a simple shear spectral model to produce some estimates of the mean-square velocity difference over given values of Δz. The distortion of a fluid region (a wake cross section, say) of dimension L is clearly due to velocity differences over Δz equal to L and smaller. In this note we explore the behavior of velocity differences over Δz with a simple model for the shear spectral density function.

DD FORM 1 JAN 73 1473 EDITION OF 1 NOV 65 IS OBSOLETE
S/N 0102-LF-014-6601

408404

SECURITY CLASSIFICATION OF THIS PAGE (When Data Entered)

TABLE OF CONTENTS

Section		Page
1	INTRODUCTION.	1
2	FORMULATION	1
3	RESULTS	5
4	DISCUSSION	7
	REFERENCES.	R-1

1.0 INTRODUCTION

It is possible to use a simple shear spectral model to produce some estimates of the mean-square velocity difference over given values of Δz. The distortion of a fluid region (a wake cross section, say) of dimension L is clearly due to velocity differences over Δz equal to L and smaller. In this note we explore the behavior of velocity differences over Δz with a simple model for the shear spectral density function.

2.0 FORMULATION

We represent the horizontal velocity field as a Fourier integral

$$\underline{u}(z) = \int_{-\infty}^{\infty} d\beta \; \underline{U}(\beta) \exp(i\beta z) \tag{1}$$

where $\underline{u}$ is the horizontal velocity vector, $\underline{U}(\beta)$ is the Fourier component amplitude (complex) vector $(U(\beta), V(\beta))$, and β is the vertical wavenumber. It is straightforward to show that

$$\langle |\underline{u}(z+\Delta z) - \underline{u}(z)|^2 \rangle = \int_{-\infty}^{\infty} d\beta \; 4 \langle U(\beta) U^*(\beta) \rangle \times (1 - \cos\beta\Delta z) \;, \tag{2}$$

where the braces indicate ensemble averaging.

From (1) it is apparent that

$$E(\beta) = 2 \langle U(\beta) U^*(\beta) \rangle \tag{3}$$

is the horizontal kinetic energy wavenumber spectral density function (defined over positive β). Using a trigonometric half-angle formula we can write (2) as

$$\langle |\underline{u}(z+\Delta z) - \underline{u}(z)|^2 \rangle = 4 \int_0^\infty d\beta \; E(\beta) \sin^2(\tfrac{1}{2}\beta \Delta z) \quad . \tag{4}$$

If we take the limit $\Delta z \to 0$ we obtain

$$\lim_{\Delta z \to 0} \left[\langle |\underline{u}(z+\Delta z) - \underline{u}(z)|^2 \rangle \Delta z^{-2} \right] = \int_0^\infty d\beta \; \beta^2 E(\beta) \tag{5}$$

where the left side of the equality is the mean-square vertical shear S^2. Equation (5) demonstrates the relationship between the spectral density of a quantity and that of its gradient. In this case

$$\phi_s(\beta) = \beta^2 E(\beta) \tag{6}$$

where $\phi_s(\beta)$ is the shear vertical wavenumber spectral density function. Relationship (6) is only applicable in the limit $\Delta z \to 0$. In general

$$\phi_s(\beta; \Delta z) = 4 \Delta z^{-2} E(\beta) \sin^2(\tfrac{1}{2}\beta \Delta z) \tag{7}$$

where $\phi_s(\beta; \Delta z)$ is the spectral density of shear defined as the mean-square velocity differences over Δz, divided by Δz^2.

Gargett et al. (1980) have assembled a shear spectrum $\phi_2(\beta)$ which we model as shown in Figure 1. The spectrum is flat to about 10 cpm where it takes a -1 slope to about 1 cpm. A high-wavenumber turbulence dissipation range exists beyond that point. We do not include contributions from that range in this analysis. We represent the spectrum as

$$\phi_2(\beta) = \phi_0 \quad , \quad \beta \leq \beta_* \quad ,$$

and

$$= \phi_0 \beta_*/\beta \quad , \quad \beta_c \leq \beta < \beta_* \quad , \qquad (8)$$

$$= 0 \qquad \beta_* < \beta \quad ,$$

where

$$\beta_* = 2\pi \times 10^{-1} \text{ rad m}^{-1} \quad (10 \text{ cpm})$$

and

$$\beta_c = 2\pi \text{ rad m}^{-1} \quad (1 \text{ cpm}) \quad .$$

We substitute (6) and (8) into (4) and define to obtain

(9a)

where

$$I_1(y_*) = \int_0^{y_*} dy \; y^{-2} \sin^2 y \quad , \qquad (9b)$$

$$I_2(y_*, y_c) = \int_{y_*}^{y_c} dy \; y^{-3} \sin^2 y \quad , \qquad (9c)$$

and $y_* = \frac{1}{2} B_* \Delta z$ and $y_c = \frac{1}{2} B_c \Delta z$. We integrate I_1 and I_2 to obtain

$$I_1(y_*) = \tfrac{1}{2} y_*^{-1} (\cos 2y_* - 1) + Si(2y_*) , \tag{10a}$$

$$\begin{aligned} I_2(y_*, y_c) = \tfrac{1}{4} \big[& y_c^{-2} (\cos 2y_c - 1) - 2y_c^{-1} \sin 2y_c \\ & - y_*^{-2} (\cos 2y_* - 1) + 2y_*^{-1} \sin 2y_* \big] \\ & - Ci(2y_*) + Ci(2y_c) , \end{aligned} \tag{10b}$$

where

$$Si(x) = \int_0^x dt\, t^{-1} \sin t \tag{10c}$$

and

$$Ci(x) = - \int_x^\infty dt\, t^{-1} \cos t \tag{10d}$$

are the sine and cosine integrals which are available in tabular form.

3.0 RESULTS

Given a value of Δz, equations (9) and (10) yield an estimate of the mean-square velocity difference as a function of the spectral amplitude ϕ_0. We have computed a number of estimates of $\frac{1}{2}\phi_0^{-1} \langle |\Delta \underline{u}|^2 \rangle$ which are shown in Table 1, and are plotted in Figure 2. A linear trend is evident for Δz greater than about 5m. The mean-square velocity difference over 16m is about 12 times the differences over 2m; the root-mean-square difference over 16m (which might be used to characterize the distortion rate) is about 3.5 times the values over 2m. Table 1 also shows

Table 1 Mean-square velocity differences versus spacing Δz. Entry with subscript $\beta < \tilde{\beta}$ refers to mean-square difference due to contributions of components with wavelengths larger than $2\Delta z$. r is the ratio of this mean-square difference to the mean-square difference with all wavenumbers contributing.

Δz(m)	$\frac{1}{2}\phi_0^{-1}\langle\lvert\Delta u\rvert^2\rangle$	$\frac{1}{2}(\phi_0\Delta z)^{-1}\langle\lvert\Delta u\rvert^2\rangle$	$\frac{1}{2}(\phi_0\Delta z)^{-1}\langle\lvert\Delta u\rvert^2\rangle_{\beta<\tilde{\beta}}$	r
2	2.14	1.072	1.00	0.93
4	5.47	1.367	1.20	0.88
5	7.10	1.419	1.22	0.86
8	11.78	1.473	1.22	0.83
10	14.90	1.490	1.22	0.82
16	24.24	1.515	1.22	0.80

$\frac{1}{2}(\phi_0 \Delta z)^{-1} \langle |\Delta \underline{u}|^2 \rangle$ which clearly approaches an asymptotic value of about 1.52. Note that $\langle |\Delta \underline{u}|^2 \rangle \propto \Delta z$ for large Δz. This implies that $S^2(\Delta z) \propto \Delta z^{-1}$: we observe this sort of behavior in the YVETTE shear estimates.

In order to characterize the contribution of components with vertical wavenumbers less than any given value $\tilde{\beta}$ to the mean-square velocity difference, (which we will denote as $\langle |\Delta \underline{u}|^2 \rangle_{\beta < \tilde{\beta}}$, we simply repeat the above analysis but with the upper limit of integration in (4) set to $\tilde{\beta}$. Of special interest might be the contribution to the mean-square velocity difference over Δz due to components with vertical scales greater than Δz. We define $\tilde{\beta} = \pi/\Delta z$ which means that we are considering the contributions to the mean-square velocity difference of components with wavelengths $2\pi \tilde{\beta}^{-1} = 2\Delta z$ and longer.

The results of these calculations are also shown in the table (column 4). The value of $\frac{1}{2}(\phi_0 \Delta z)^{-1} \langle |\Delta \underline{u}|^2 \rangle_{\beta < \tilde{\beta}}$ approaches an asymptotic value of 1.22. Also shown in the table is the ratio

$$r = \langle |\Delta \underline{u}|^2 \rangle_{\beta < \tilde{\beta}} \Big/ \langle |\Delta \underline{u}|^2 \rangle .$$

The results show that 93% of the mean-square velocity difference over 2m is due to components with wavelengths of 4m and longer. This value drops to asymptotically about 80%.

4.0 DISCUSSION AND A SIMPLE SIMULATION

These results, which are based on a spectral-density-function model, suggest that the mean-square velocity difference over values of Δz in our range of interest increase roughly as Δz and that $S^2(\Delta z) \equiv \langle |\Delta \underline{u}|^2 \rangle \Delta z^{-2}$ behaves as Δz^{-1}. Trends of this sort are evident in YVETTE data. If we characterize the relative distortion rate between locations Δz apart as $\langle |\Delta \underline{u}|^2 \rangle^{\frac{1}{2}}$, we see that the distortion rate behaves as $\Delta z^{1/2}$. This implies that the treatment of velocity variation as a linear variation over scales of interest, for wake model application say, may be inappropriate. However, 90% or better of the root-mean-square distortion rate of two points separated by Δz is given by components with wavelengths $2\Delta z$ and longer. This means that while we can adequately characterize the distortion rate between two points separated by Δz with velocity data resolved to wavelengths of $2\Delta z$ and longer, we should not characterize the distortion between these locations with a linear variation.

In an attempt to make these results more vivid, we undertook an elementary kinematic "wake" simulation using the velocity field recorded during YVETTE deployment 09 in the Western Sargasso (Lambert et al., 1980). The velocity profile is shown in Figure 3; the data have an effective resolution of about 3m. We computed the distortion of initially nearly circular (10m diameter) patterns of passive tracers located in depth intervals 70-80m, 110-120m, 220-230m, 345-355m, with the velocity field fixed over the simulation time interval. The resulting "wake" cross-sections to one-hour time-late are shown in Figure 4.

In three of the four cases, there clearly is substantial distortion over scales less than the initial wake cross section.

Finally, we note that the work of Patterson et al. (1981) with YVETTE data suggests that $\overline{S^2(\Delta z = 2m)} \approx \overline{N^2}$, where $\overline{N^2}$ is the mean (depth averaged) Brunt-Väisälä frequency. If the spectral shear representation is appropriate we can estimate S^2 over other Δz via (9) and the estimate of ϕ_o given $S^2(\Delta z = 2m)$.

SHEAR SPECTRAL MODEL AND CORRESPONDING
MEAN-SQUARE VELOCITY DIFFERENCE OVER ΔZ

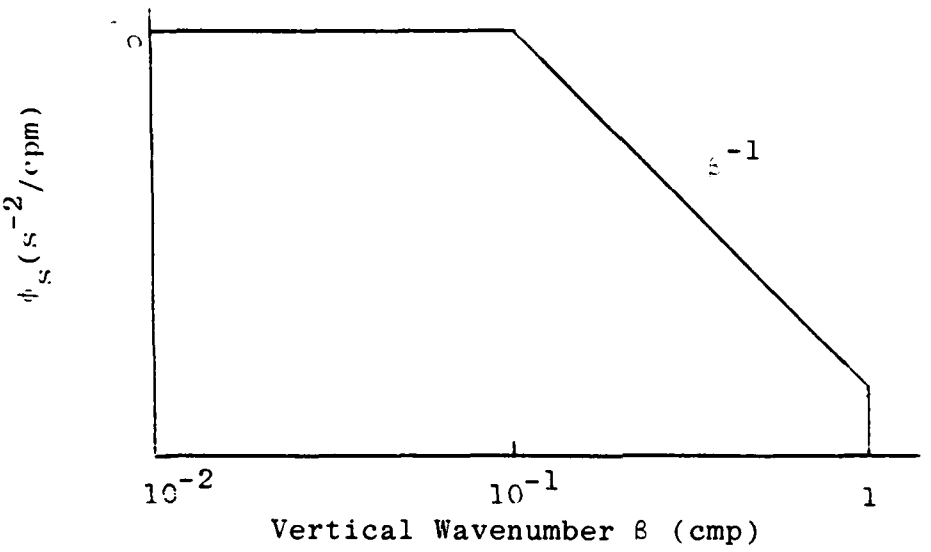

Figure 1 Shear Spectral Model After Gargett et al. (1980)

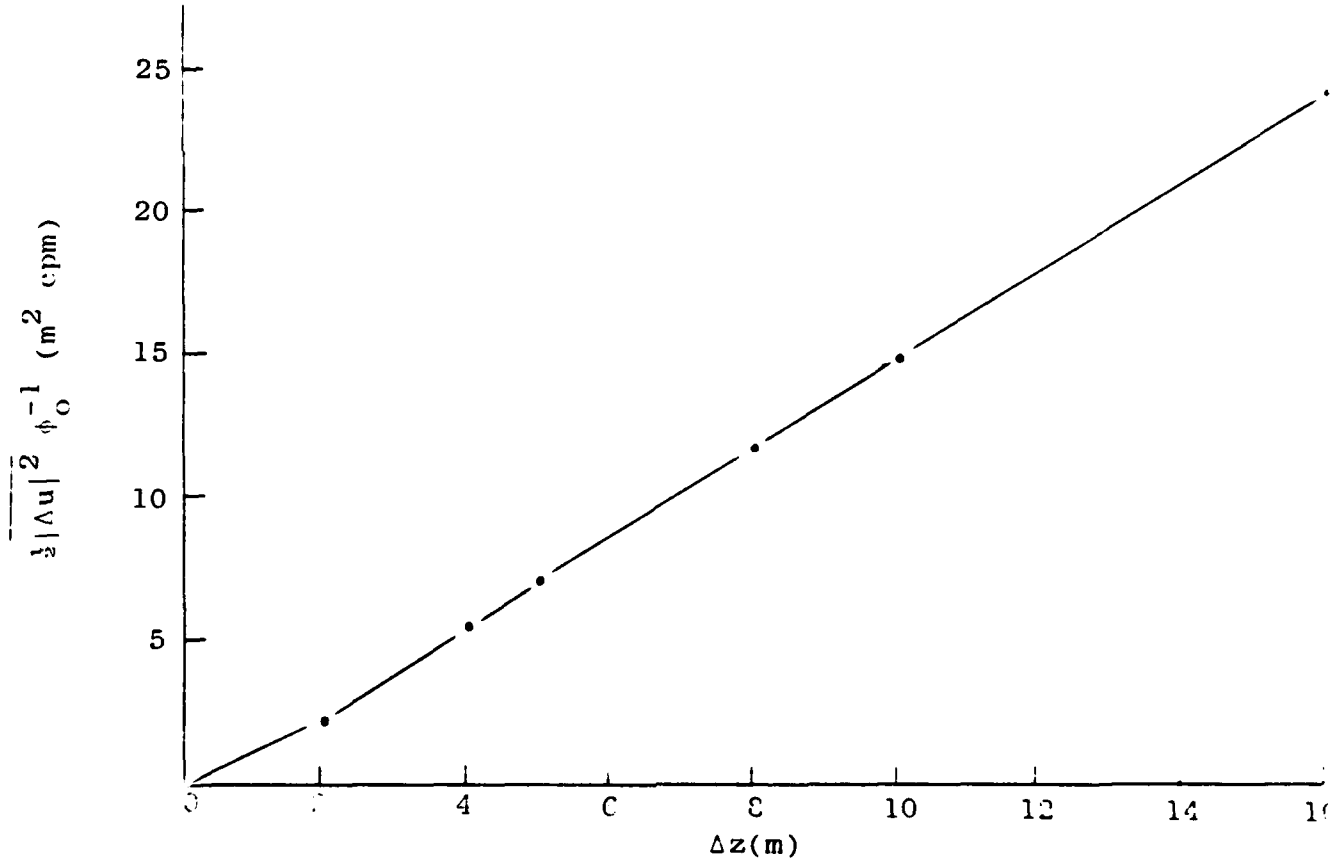

Figure 2 Mean-Square Velocity Difference Over Δz.

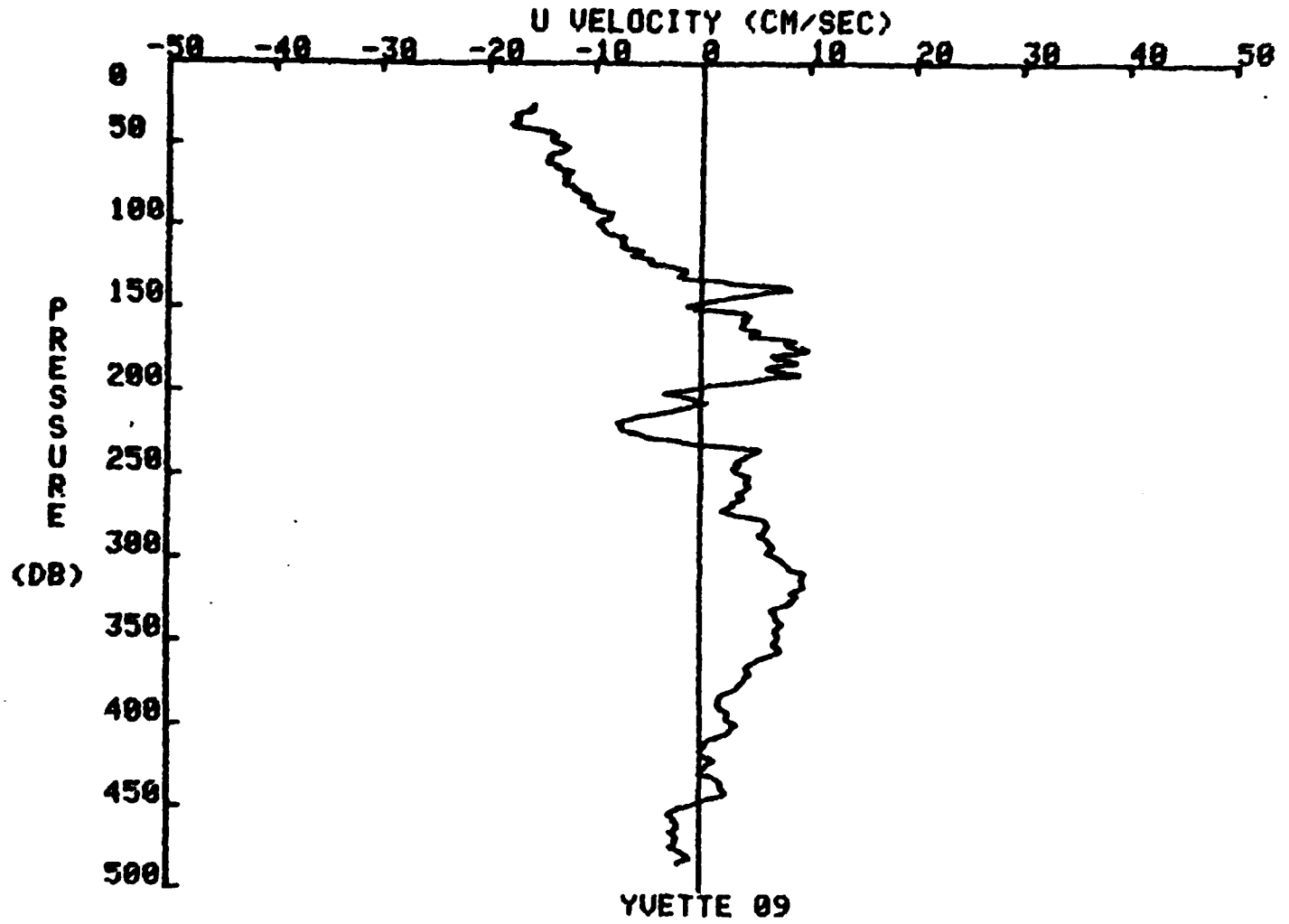

Figure 3 YVETTE 09 Velocity Profile used for Simulations

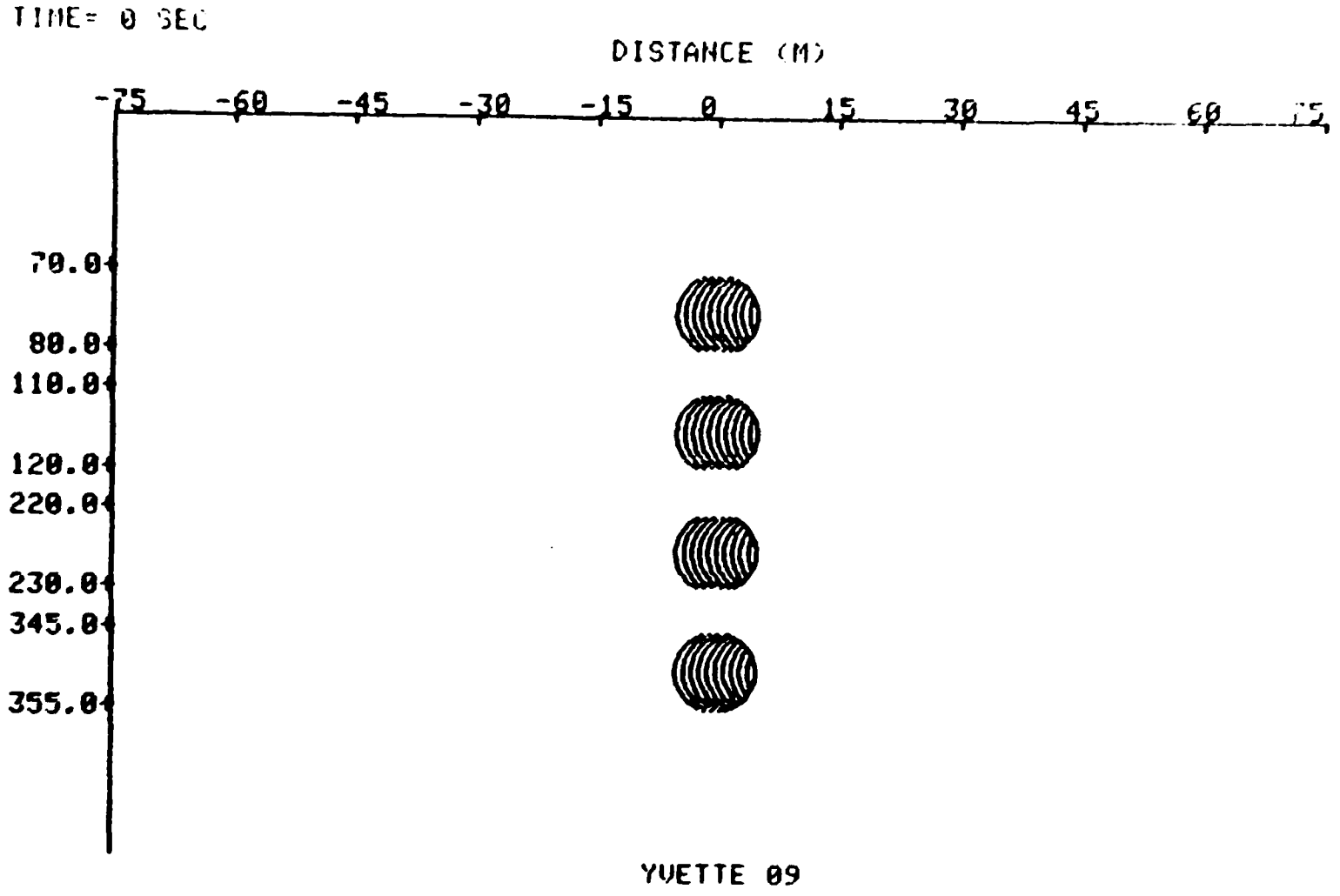

Figure 4 Distortion of nearly circular pattern of passive tracers in YVETTE 09 velocity field. Note the discontinuous vertical scale.
(a) Initial Pattern

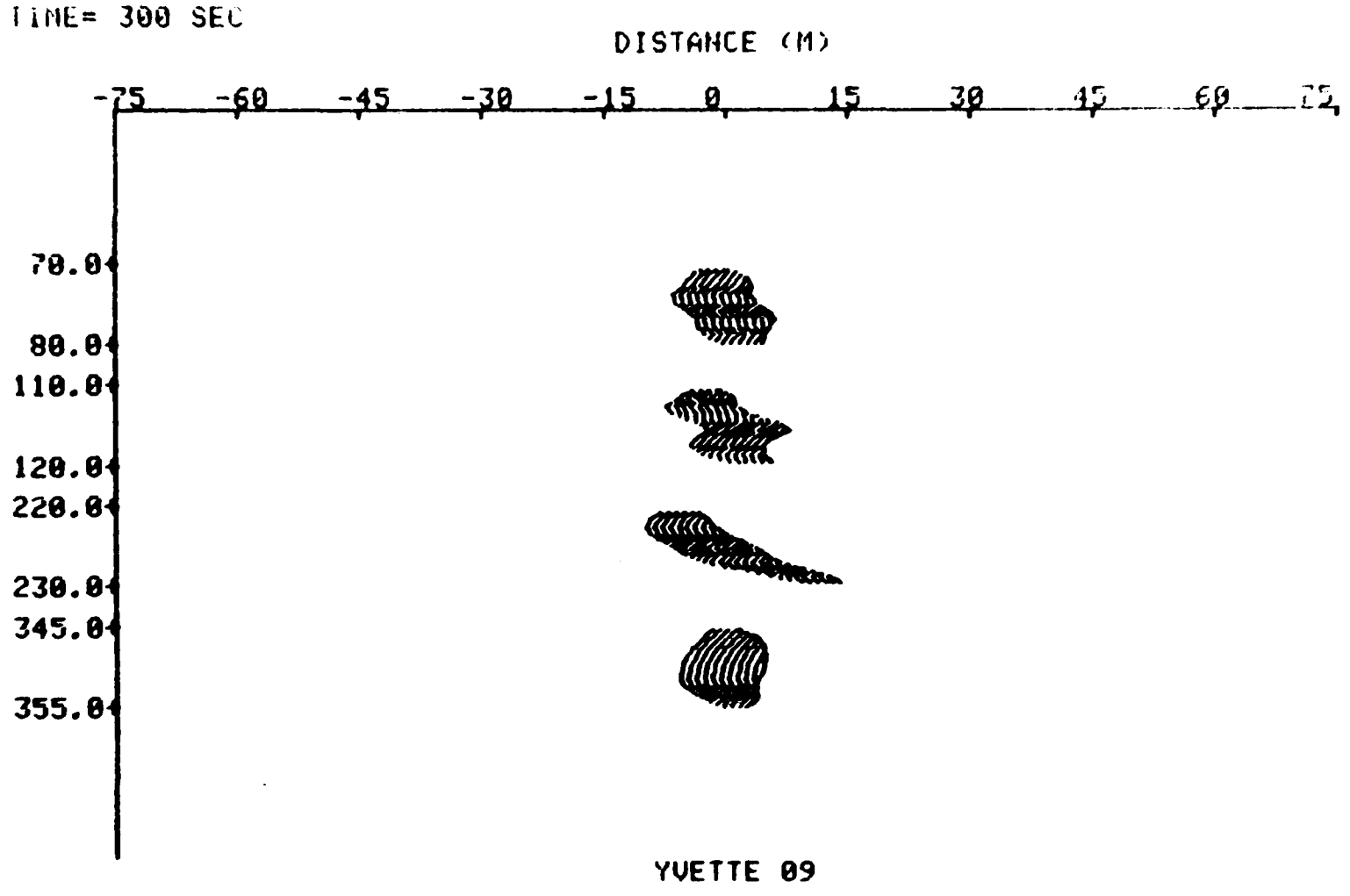

Figure 4(b) Pattern after 5 minutes

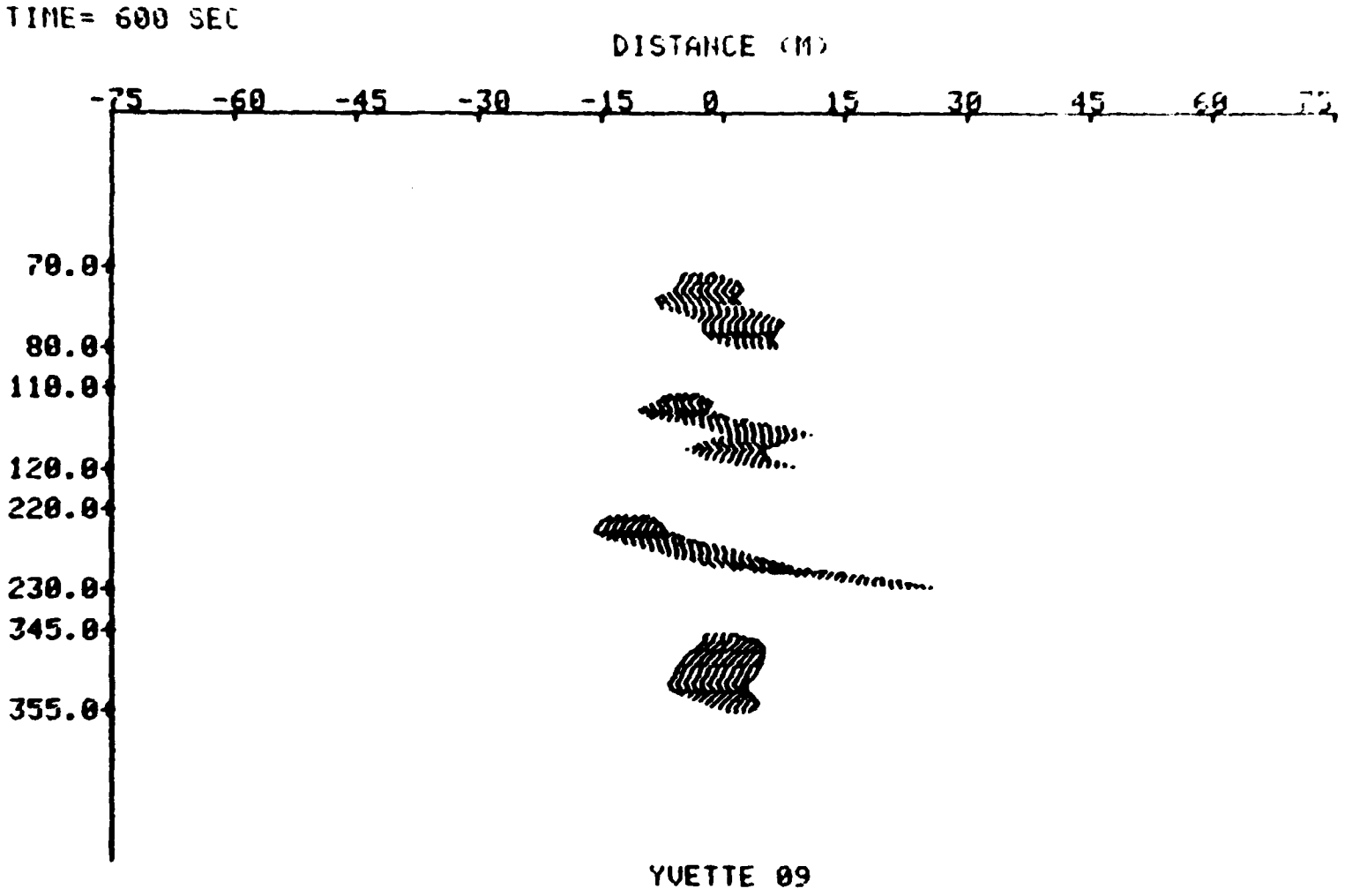

Figure 4(c) Pattern after 10 minutes

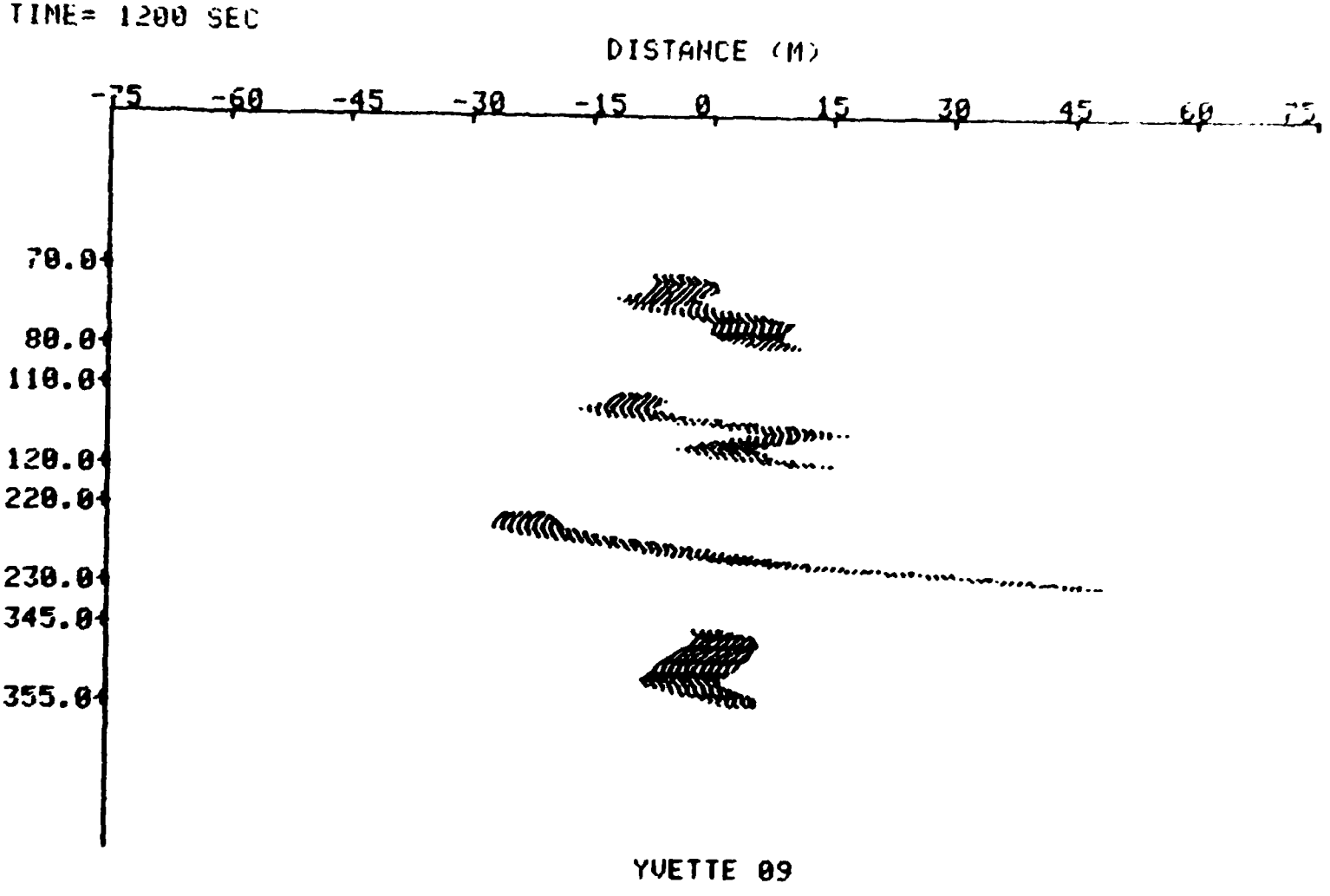

Figure 4(d) Pattern after 20 minutes

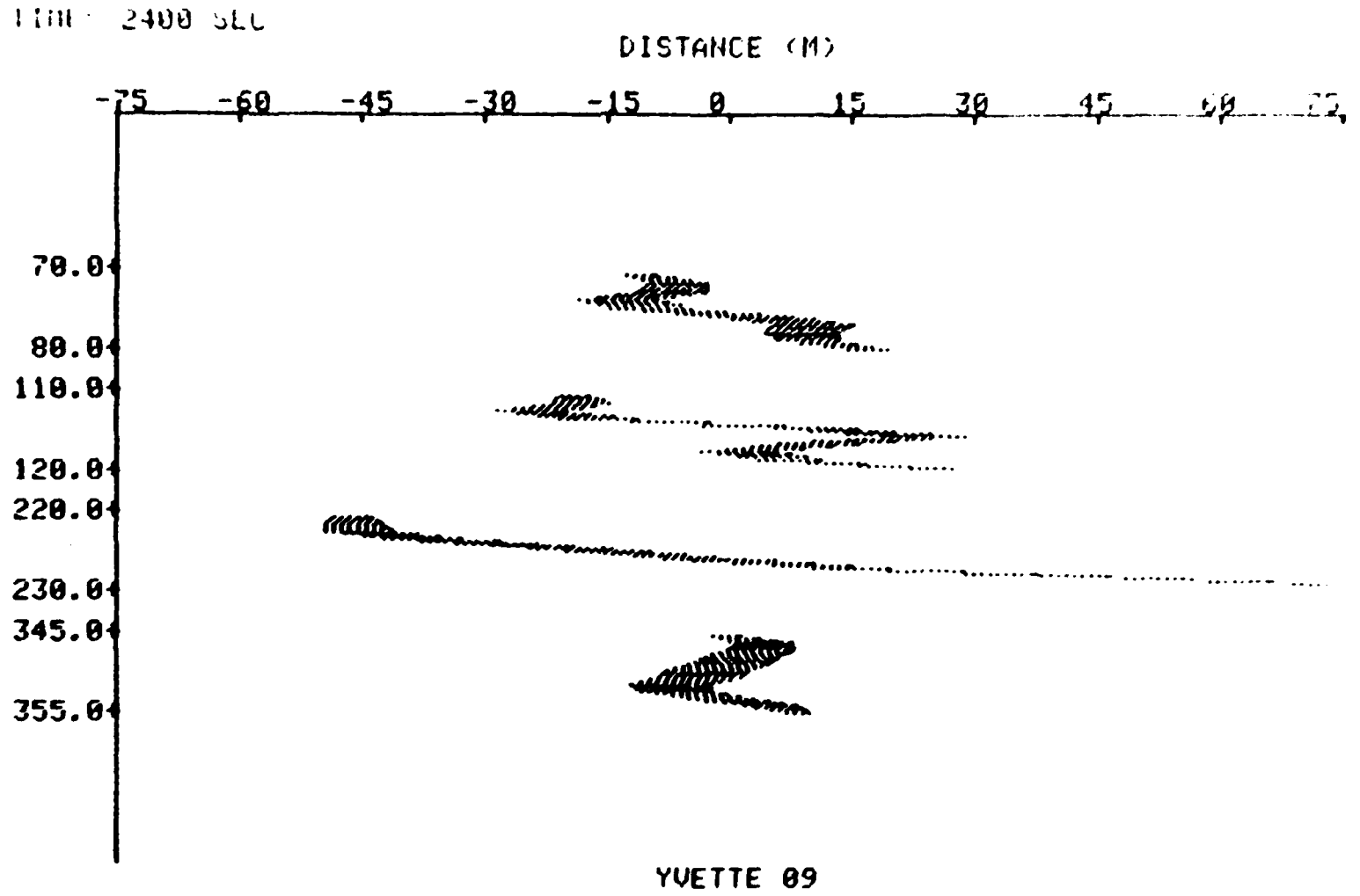

Figure 4(e) Pattern after 40 minutes

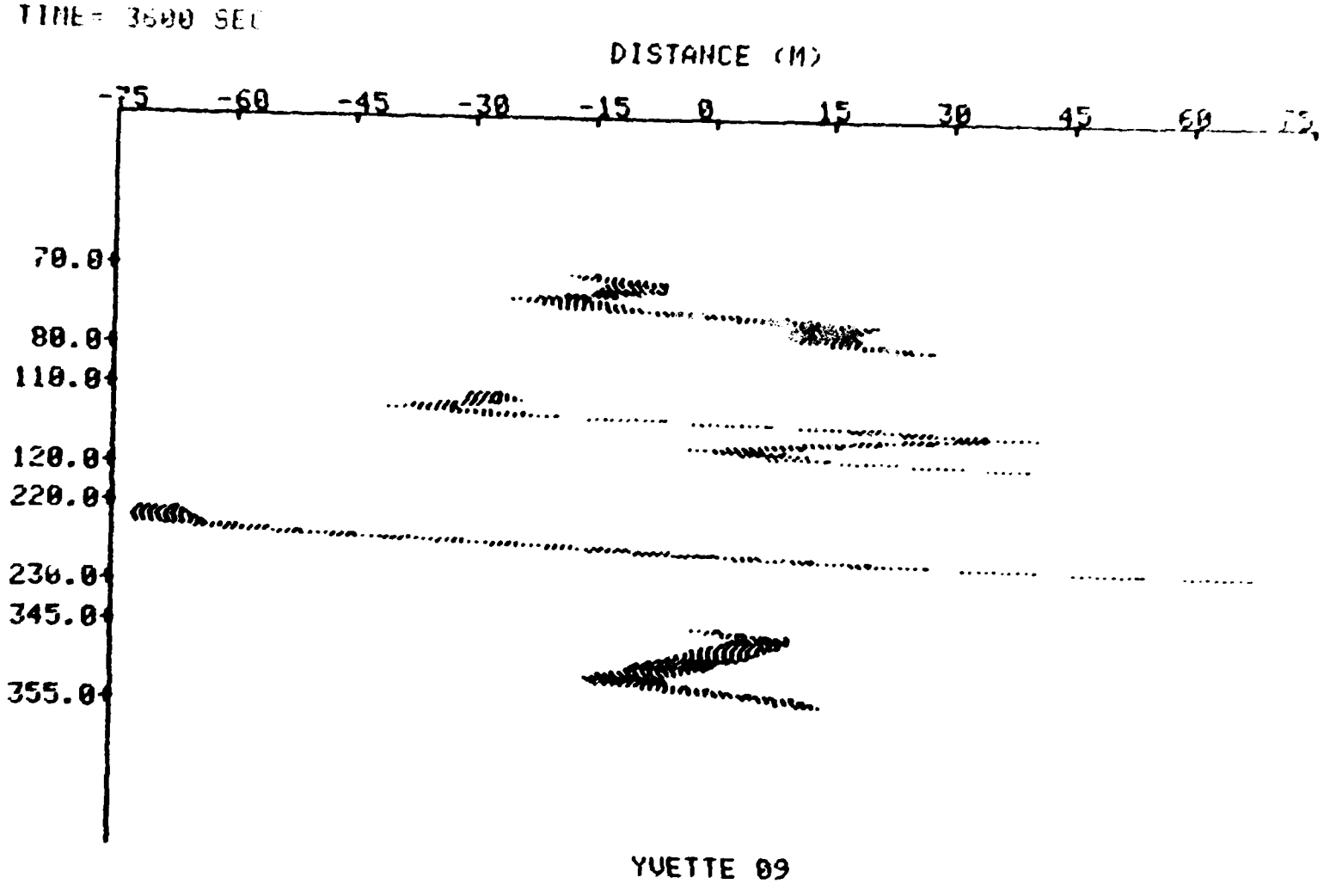

Figure 4(f) Pattern after 60 minutes

REFERENCES

Gargett, A. E., P. J. Hendricks, T. B. Sanford, T. R. Osborn, and A. J. Williams III (1980): A composite spectrum of vertical shear in the upper ocean from the profilers EMVP, SCIMP and CAMEL, Pacific Marine Science Report 80-11, Institute of Ocean Science, Sidney, B. C.

Lambert, R. B., Jr., D. L. Evans and P. J. Hendricks, 1980: Data Report-SCIMP and YVETTE, Progres Report I, Ocean Physics Div. Tech Rept. 80-201-04, Science Applications, Inc., McLean, VA.

Patterson, S. L., F. C. Newman, D. M. Rubenstein and R. B. Lambert, Jr. (1981): Spatial distribution of vertical shear, SAI Technical Report 81-201-02, Science Applications, Inc.

NORDA DISTRIBUTION LIST FOR

REPORT NO. SAI-82-485-WA

ENTITLED "SPECTRAL MODEL PREDICTIONS OF

MEAN-SQUARE-SHEAR DISTORTION RATES"

Naval Ocean Research and
Development Activity
Code 100, 110, 300, 320,
330, 340, 350, 360
(one copy each)
NSTL Station, MI 39529

Naval Ocean Research and
Development Activity
Code 540
NSTL Station, MI 39529 (5)

NORDA Liaison Office
800 N. Quincy St., Rm. 502
Arlington, VA 22217 (1)

Office of Naval Research
Code 102O
800 North Quincy Street
Arlington, VA 22217
ATTN: Dr. R. Winokur (1)

Office of Naval Research
Code 103T
800 North Quincy Street
Arlington, VA 22217
ATTN: Dr. S. G. Reid (1)

Office of Naval Research
Code 480
800 North Quincy Street
Arlington, VA 22217
ATTN: Dr. L. Goodman (1)

Commander
Naval Oceanography Command
NSTL Station, MS 39529 (1)

Dr. A. Andreassen
OP-95T
Pentagon
Washington, D.C. 20350 (1)

Chief of Naval Operations
Department of the Navy
OP-952
Washington, D.C. 20350
ATTN: CDR Harlett (2)

CAPT H. E. Marxer
OP-212E
Pentagon
Washington, D.C. 20350 (1)

Commanding Officer
Naval Research Laboratory
Washington, D.C. 20375 (1)

Naval Research Laboratory
Code 4340
Washington, D.C. 20375 (1)

Commanding Officer
Naval Oceanographic Office
NSTL Station, MS 39529 (1)

Naval Oceanographic Office
Code 7004
NSTL Station, MS 39529 (1)

Naval Oceanographic Office
Code 7200
NSTL Station, MS 39529 (1)

Commanding Officer
Naval Ocean Systems Center
San Diego, CA 92152 (1)

Naval Electronics Systems Command
Code 320
Washington, D.C. 20360 (1)

Naval Electronics Systems Command
PME 124
Washington, D.C. 20360 (1)

Dr. W. Welch
TRIDENT Systems Project Office
National Center 3
Room 7W66
Washington, D.C. 20360 (1)

Dr. G. D. Smith
Applied Physics Laboratory
The Johns Hopkins University
Johns Hopkins Road
Laurel, MD 20810 (1)

Dr. L. J. Smith
Applied Physics Laboratory
The Johns Hopkins University
Johns Hopkins Road
Laurel, MD 20810 (1)

Dr. G. E. Merritt
Applied Physics Laboratory
The Johns Hopkins University
Johns Hopkins Road
Laurel, MD 20810 (1)

Dr. H. E. Gilreath
Applied Physics Laboratory
The Johns Hopkins University
Johns Hopkins Road
Laurel, MD 20810 (1)

Dr. R. Hoglund
Office, Assistant Sec. of Navy
Pentagon
Room 4-D745
Washington, D.C. 20350 (1)

Dr. P. A. Selwyn
Strategic Support Projects Office
SP-2023
Department of the Navy
Washington, D.C. 20376 (1)

Dr. Melbourne G. Briscoe
Woods Hole Oceanographic Inst.
Woods Hole, MA 02543

Dr. T. Sanford
University of Washington
Applied Physics Laboratory
1013 NE Fortieth Street
Seattle, WA 98195 (1)

Naval Intelligence Support Center
Code 600
4301 Suitland Road
Washington, D.C. 20390 (1)

Naval Underwater Systems Center
New London Laboratory
Code 60
New London, CT 06320 (1)

Administrative Contracting Officer
Defense Contract Administration Services
Management Area - San Diego
Code S0514A
Bldg. 4, AF Plant 19, 4297 Pacific Hwy.
San Diego, CA 92110 (1)

Director
Naval Research Laboratory
Code 2627
Washington, D.C. 20375 (6)

Defense Technical Information Center
Code S47031
Bldg. 5, Cameron Station
Alexandria, VA 22314 (12)

Office of Naval Research
Code N62887
Western Regional Office
1030 E. Green Street
Pasadena, CA 91106 (1)


FILME
8